Solid-state Detectors

4

Development Journey of Eu^{2+} doped LiI Single Crystal Based Portable Solid-state Detectors for Thermal Neutrons

Awadh Singh*, M. Tyagi, S. G. Singh, G. D. Patra, D. S. Sisodiya, Sonu and Shashwati Sen

Technical Physics Division, Bhabha Atomic Research Centre (BARC), Trombay – 400085, INDIA

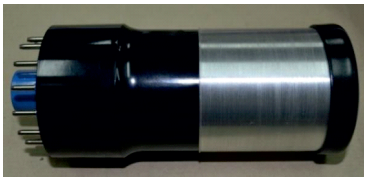

A hermetic sealed LiI:Eu detector

ABSTRACT

Single crystals of Eu-doped LiI are well known for their potential applications to be used as a scintillator to detect thermal neutrons. However, the growth of these single crystals are challenging due to their hygroscopic nature, sticking to the crucible and inclusions. We have successfully addressed all these problems for the growth of single crystals of LiI: Eu. Detectors fabricated from these in-house grown crystals were used in the Pulse height measurements for thermal neutrons.

KEYWORDS: *Crystal growth, Scintillator, Neutron Detector, Thermal Neutrons*

Introduction

Neutron detectors serve a wide range of applications, spanning research, defense, security, and nuclear industries. Conventional neutron detectors utilizing gas-based systems, predominantly rely on ^{3}He and BF_3 gases, exhibit suboptimal efficiency levels. Poor gamma discrimination, wall effect are some of the challenges which limits the applications of the gas based thermal neutron detectors in the field applications [1,2]. In contrast, europium- activated lithium iodide emerges as a well- established scintillator with particular utility in thermal neutron detection. The deployment of europium-doped lithium iodide in single crystal form bestows substantial advantages, including higher detection efficiency, as well as enhanced portability and compactness compared to gas-based detectors. Moreover, its capability to detect both gamma rays and thermal neutrons extends its application scope. In europium-doped lithium iodide (LiI: Eu), the naturally occurring isotope ^{6}Li is endowed with a significant absorption cross-section(^{3}~940 barns) for thermal neutrons. Consequently, this is instrumental in a 'Q' value energy of 4.8 MeV effectively getting deposited within the scintillator [1]. This inherent characteristic facilitates robust pulse height differentiation between low-energy gamma radiation and thermal neutrons. Upon the engagement of thermal neutron with ^{6}Li leading to (n, α) ^{3}H reactions, the produced charged particles excite the Eu^{2+} ^{1}ions, inducing a scintillating emission lasting a few microseconds within the blue region (~470 nm) of the electromagnetic spectrum. This emission profile harmonizes seamlessly with the responsiveness of Bialkali photomultiplier tubes(PMTs), thus rendering standard pulse processing electronics comprising pre amplifiers, shaping amplifiers, and Multi-channel analyzers (MCA) for the readout purposes [1,3].

However, it's essential to acknowledge that the hygroscopic tendencies of lithium iodide impart a significant dependence of the crystal's scintillation property on growth processes. Consequently, a challenge arises in maintaining consistent scintillation responses across single crystals originating from the same charge, unless the entirety of the growth procedure is meticulously optimized. To address this, the present paper delves into a comprehensive discourse on the recipe of the single crystal growth procedure and the detector fabrication for the thermal neutron detectors employing lithium iodide single crystals at its heart.

Experimental

Single crystals of Lithium Iodide doped with 0.1% Europium (LiI:Eu) were successfully grown utilizing the Bridgman technique. The growth procedure involved using high- purity, anhydrous LiI and EuI_2, enclosed within a quartz ampoule under an argon atmosphere. Specially designed quartz crucibles are prepared through etching with a 10% HF solution for 5-7 minutes, followed by baking at 700 degrees Celsius for 10 hours under rotary vacuum conditions. The prepared crucible was transferred into a glove box through a right-angle valve under vacuum conditions, assuring an oxygen and moisture content of less than 0.1 ppm. The initial charge comprised ultra-dry anhydrous beads of LiI (^{6}Li with a natural abundance of 7.4%) and EuI_2, both possessing a purity of 99.99%. These components were combined in a stoichiometric ratio to have a 0.2 mole% doping of Eu in the LiI matrix. Subsequently, the mixture was subjected to dehydration within the quartz ampoule at 300^{0}C for a span of 4 hours under a running vacuum of 5 x 10^{-5} mbar to eliminate any residual moisture or oxygen. The sealing of the quartz ampoule was ultimately executed under a continuous vacuum. This sealed ampoule was then positioned within a Bridgman furnace, wherein it was heated to 510^{0}C and maintained at this temperature for 4 hours to achieve thermal equilibrium in the melt. The process of single crystal growth initiated as the ampoule was gradually lowered through a temperature gradient of approximately 12-15 K/cm. This lowering procedure consisted of an initial phase at a rate of 0.2 mm/h within the cone region, followed by a rate of 0.5 mm/h in the

*Author for Correspondence: Awadh Singh
E-mail: awadhks@barc.gov.in

Fig.1: A typical Bridgman Crystal Growth Furnace.

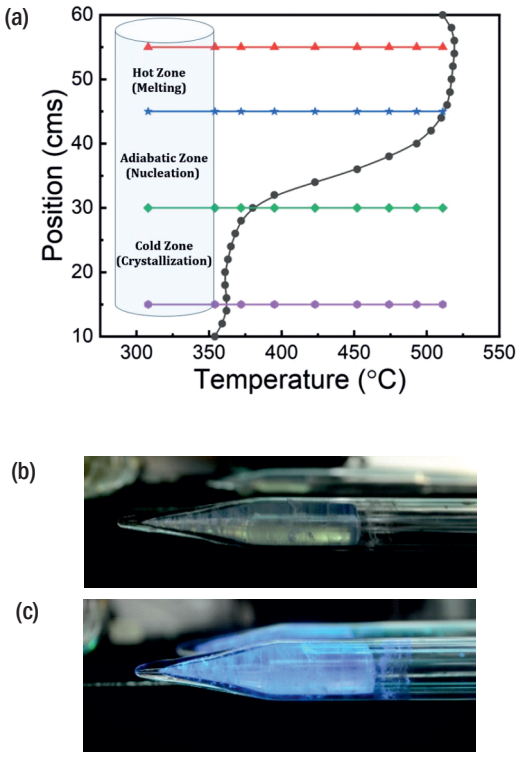

Fig.2 (a):Temperature gradient profile used for the growth of LiI:Eu^{2+}. (b) As grown single crystal inside quartz ampoule. (c) As grown single crystal inside quartz ampoule under UV radiation.

cylindrical region. Upon the completion of crystal growth, the quartz ampoule housing the grown single crystal subjected to a 10-hour annealing at 450°C. This annealing step aimed to mitigate thermal stresses in the crystal arising from contact between quartz and crystal. Subsequently, the grown crystals were gradually cooled down to room temperature at a controlled rate of 10-15°C per hour. To retrieve the grown single crystals, the quartz crucible was dissected under the protection of silicon oil. This approach was taken to prevent any potential contact with moisture or oxygen, which could compromise the single crystal's properties. The structural characteristics of the grown crystals were studied using Powder XRD and the powder samples were wrapped in a kapton sheet to protect the samples from oxygen and moisture during the data collection. The samples were found to be chemically stable during and even after the measurements for few hours. For the optical and scintillation measurements, the samples were prepared from the as-grown single crystals within the glove box. The Radio-luminescence (RL) properties were evaluated using a monochromator with compatible software (Princeton Instruments Acton spectrapro SP-2300). For excitation, a white X-ray source with a Cu target, operating at an accelerating voltage of 40 kV and a tube current of 30 mA, was employed. Scintillation measurements were performed on a processed scintillator measuring 10 mm, 25 mm and 50 mm in diameter and 2 mm approx. in thickness. This scintillator was hermetically sealed within a cylindrical aluminum container, with a high-purity quartz plate on one end. A diffused reflector (Al_2O_3) was incorporated in the aluminum container to facilitate efficient light collection from the quartz plate. Ultimately, a Hamamatsu PMT was coupled to the LiI: Eu scintillator for thermal neutron measurements.

Results and Discussion

Fig.1 shows the photograph of the Bridgman furnace designed by CTS, TPD and fabricated with the help of the local industry for the single crystal growth of low temperature halide single crystals. The gradient of the furnace with two isothermal zones operating at the melting temperatures and separated by an adiabatic zone created by the baffle has been shown Fig.2. 4N pure LiI and EuI_2 (Source: Lanhit) were used for carrying out the single crystal growth experiments. A freshly grown single crystal of Lithium Iodide doped with 0.1% molar concentration of Europium grown using the Bridgman furnace developed at CTS, TPD is shown in Fig.2b. The single ingot exhibits a pristine, crack-free structure without any observable defects and crack-free structure. The same crystal under UV light is shown in Fig.2c. and shows strong luminescence in the blue region.

The single crystals were grown with a lowering rate of 0.1 mm/hr in the nucleation region and the lowering rate was varied in the range of 0.2 mm to 0.5 mm per hour in the cylindrical region. It has been found that if the material dehydration is good which is observed directly from the vacuum during dehydration a higher pull rate up to 0.5 mm/hr for crystal up to 1-inch diameter can be employed. However, the dehydration for less than 4 hours and temperatures below 300°C leads to inclusions in the grown crystal along the length which segregate at the end of the cylindrical region. It has also been found beneficial to dehydrate the material before the doping up to 6 hours and then dehydrate again for 2 hours after Eu^{2+} doping. However, this dehydration process is also affected by the amount of starting charge and multiple dehydration cycles were found to be beneficial if the starting charge is more than 100 g. Usually, 350 g of starting charge were loaded in a 2-inch quartz ampoule for the growth of a 2 inch diameter and 2-inch length single crystal, and required much longer dehydration time to achieve transparent single crystals. Post growth, the retrieval of the single crystal was easy in 15 mm diameter single crystals. However, the crystal growth experiments carried out for 1-inch and 2-inch diameter single crystals results in sticking to the crucible wall and cracking during or after the growth. We could address the sticking problem for the 1-inch single crystal by optimizing the

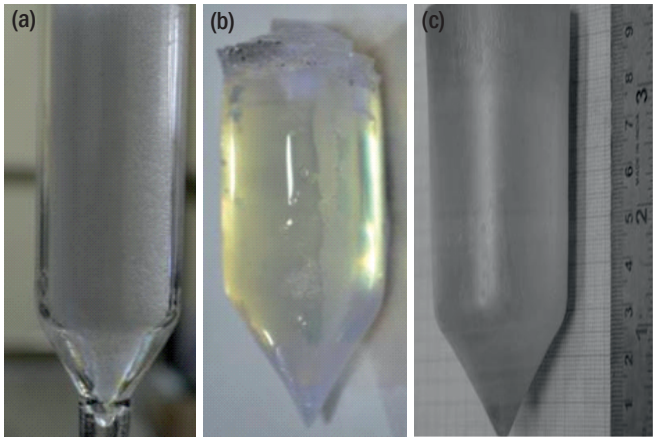

Fig.3: (a) A Quartz ampoule loaded with starting charge of LiI: Eu^{2+}. (b) A 1-inch diameter single crystal of LiI: Eu^{2+}. (c) A 2-inch diameter single crystal of LiI: Eu^{2+}.

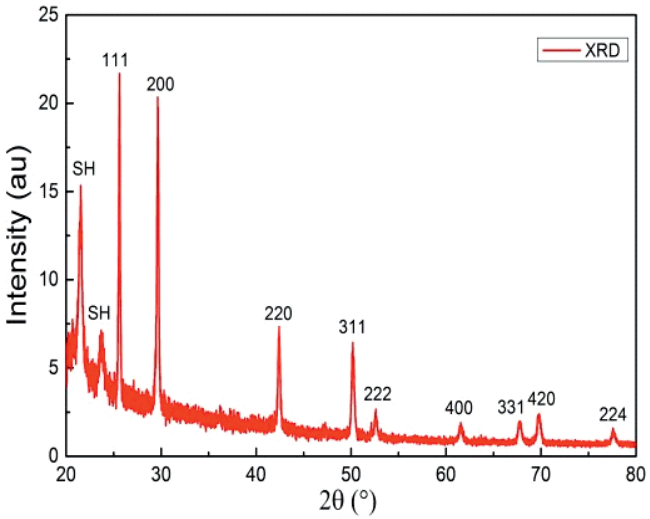

Fig.4: Powder XRD Pattern of LiI:Eu^{2+}.

dehydration time but for the 2-inch single crystals the sticking to the walls couldn't be restricted. Hence, we employed inversion technique where the whole furnace was inverted after the completion of the growth experiments and temperature were raised for the region where grown single crystal lies to melt the crystal from the surface and glide it to the region where the temperature was reduced just below melting point. The thermal shock was minimized in this process and damping mechanism were used to minimize the mechanical shock during the glide of the grown single crystal inside the crucible. We could successfully address this issue also by carrying out the crystal growth experiment in carbon coated quartz ampules and transparent and crack free single crystals were achieved for both 1-inch and 2-inch diameter. The Photographs in Fig.3a. shows the quartz ampoule loaded with LiI: Eu^{2+} while the Fig.3b and 3c. shows the as grown single crystal ingot for the 1-inch and the 2-inch diameter single crystals. We have observed core formation in the 2-inch diameter single crystal when the lowering rate was higher than 0.2-0.3 mm per hour and we couldn't completely address this issue. The non-uniform segregation of Eu^{2+} in LiI matrix along with the initial purity of the starting charge are a few possible reasons and we are addressing this issue by purifying the starting charge with multiple crystallizations.

The grown crystals were also characterized for their structural properties and the power XRD measurent were carried out in the range of 10-80^0 and the XRD pattern is shown in Fig.4. It confirms the phase of the grown crystal without any additional peaks which may have arisen due to oxygen or moisture contamination as the material is quite reactive to the moisture/oxygen at elevated temperatures. We have observed two additional peaks arising from the polythene sheets used to wrap the powder to protect it and have been marked as SH. Optical characterization was carried out on the transparent and core free region of the grown single crystals. The UV response of the same crystal is shown in Fig.5. It shows transmission of around 45% in the 450-500 nm range with ~20% reflective losses at windows surface of the sample holder. A cut off at 450 nm have been found in the transmission due to the absorption of light in the Eu^{2+} energy levels [3,4]. The radioluminescence spectrum shown in Fig.6. features a prominent emission band peaking at approximately 470 nm, accompanied by a minor tail at the higher wavelength range. This emission band aligns with electron transitions within the Eu^{2+} ions (5d ⟶ 4f) embedded in the LiI matrix. However, no discernible signatures of Eu^{3+} bands were detected [3, 5]. The comparison of transmission and radioluminescence suggests significant self-absorption in large crystal dimensions due to

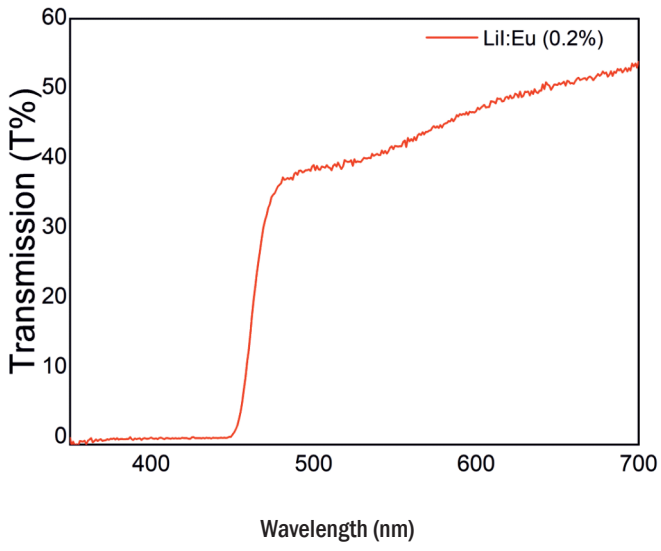

Fig.5: Transmission Spectrum of LiI:Eu^{2+}.

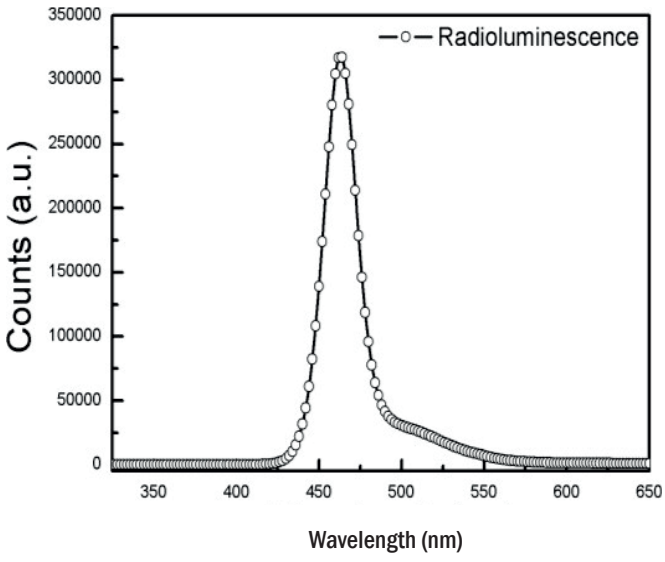

Fig.6: X-ray induced Luminescence from LiI:Eu^{2+}.

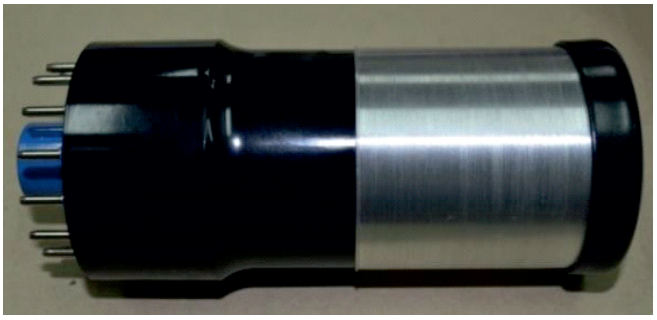

Fig.7: A hermetic sealed LiI:Eu detector.

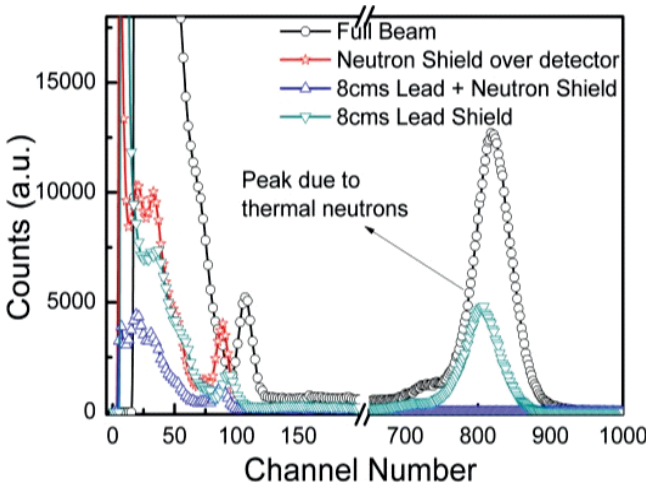

Fig.8: Pulse height spectrum due to thermal neutrons at Dhruva beam line from LiI:Eu^{2+}.

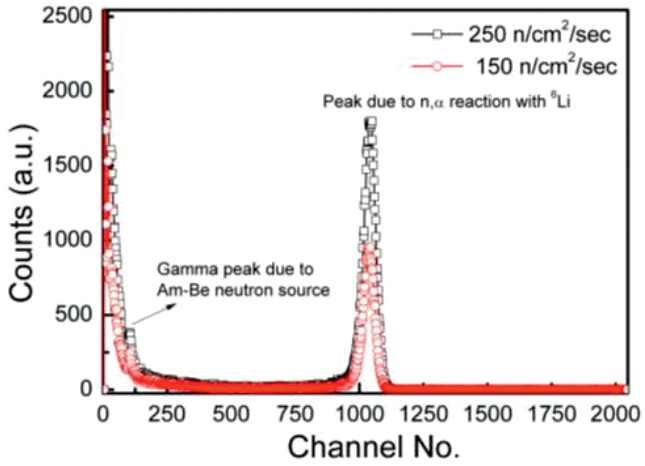

Fig.9: Pulse height spectrum due to thermal neutrons with standard flux from LiI:Eu^{2+}.

Fig.10: A USB based handheld thermal neutron detector employing LiI:Eu^{2+} single crystal.

the overlap of the transmission and the emission spectrum. The electronic properties needs tailoring to address this issue as large size crystals were required for the higher efficiency and work with co-doing in also in progress.

After studying the optical properties suitable for the scintillation application, the scintillation measurements were carried out on the detectors fabricated from the LiI: Eu^{2+} single crystals. A typical hermetically sealed LiI: Eu detector is shown in Fig.7. The pulse height spectrum originating from thermal neutrons from the Dhruva reactor has been shown in Fig.8. A ^{60}Co source was positioned proximate to the detector to discern the detector's response to both gamma and neutron energies. Notably, the spectra distinctly reveal a prominent peak occurring around channel number 850, attributed to the interaction between thermal neutrons and the ^{6}Li content within the scintillator. This interaction elicits charged particles via the [^{6}Li (n, α) ^{3}H] reaction, inducing scintillation within the crystal. To ascertain the origin of this peak, a borated envelope was employed to enclose the entire detector, leading to a reduction in counts to background levels. A lead shield used in attempt to minimize the gamma background in the reactor hall could also scatter the neutrons and height of the photo peak was found to be reduced but doesn't vanish completely. The photo peaks corresponding to gamma energies of 1.17 MeV and 1.33 MeV originating from the ^{60}Co source were indistinguishable, manifesting at approximately channel number 100. Notably, the scintillator's efficiency for gamma energies was compromised due to its low density and limited effective atomic number (Z_{eff}). However, the scintillator's proficiency in thermal neutron detection exhibited significant enhancement, with the potential for further augmentation through the enrichment of ^{6}Li in comparison to the naturally prevalent ^{7}Li. To further understand the linearity response of the LiI: Eu detector, the pulse height measurents at standard neutron flux facility were carried out. The spectrum in Fig.9 shows the response of the detector when radiated with thermal neutrons from the Am-Be Source. The spectrum distinctly portrays a photo peak corresponding to the 4.8 MeV energy deposited by charged particles resulting from their interaction with thermal neutrons. The integrated counts with 150 n/cm^2/sec and 250 n/cm^2/sec were in good agreement and exhibits the linearity in the response of the neutron flux.

However, the Pulse height spectrum recoded for large size single crystals (2-inch diameter) shows broadening of the peak which may have been originating due to the self-absorption or the impurities affecting the scintillations response of the detector [6,7]. Further experiments are in continuation to improve the detector response for the large size detectors required for the higher efficiency [8].

A hand held detector was designed and developed by CTS, TPD for field application employing the LiI: Eu^{2+} single crystal. A photograph of the detector employing a hermetically sealed LiI: Eu detector is shown is Fig.10. It has been used for long term testing for the stability of the detector over three months. Fig.11 presents the pulse height spectrum acquired from a ^{137}Cs source over a three-month interval, during which uniform signal processing parameters were maintained. Clearly discernible, the spectrum displays a photo peak situated nearly at the same channel, depicting fluctuations below 3%. These slight deviations, possibly stemming from experimental uncertainties, provide substantiation for the reliability of the observed patterns. This underscores the achievement of a secure hermetic seal connecting the scintillator and the directly coupled PMT, thereby ensuring its

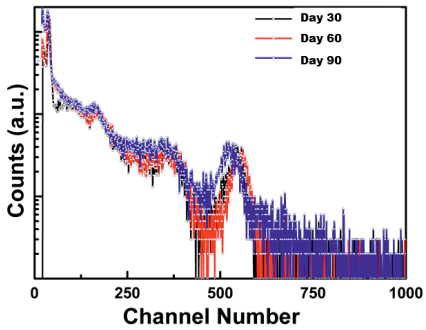

Fig.11: Pulse height spectrum due to ^{137}Cs recoded under identical settings over a period of 3 months.

resilience over an extended timeframe. Concurrently, ongoing inquiries are underway to enhance and optimize the detector's efficiency through the utilization of this hermetic sealing approach.

Conclusion

Single crystals of 0.1 % Eu doped lithium iodide were grown using Bridgman technique. Structural and optical properties show a promising journey towards the development of the high efficiency detectors for thermal neutrons. Detectors fabricated using the LiI: Eu scintillators were used for thermal neutron detection. Thermal Neutron detection has been carried out using the hermetically sealed detector and its long term performance has been evaluated.

References

[1] G.F. Knoll, Radiation Detection and Measurement, John Wiley & Sons, Second Edition, 1978.

[2] R. Cervellati and A. Kazimierski, "Wall effect in BF3 counters," Nucl. Instr. and Meth. 60, 173, 1968.

[3] Sajid Khan, et al, Nucl. Inst. And Meth. A 793 (2015) 31-34.

[4] Boatner, L.A, et al, Nucl. Inst. And Meth. A 854 (2017) 82-88.

[5] A.K. Singh et al, Proceedings of the DAE Symp. on Nucl. Phys. 63 (2018).

[6] Kazuo Suzuki, J. Phys. Soc. Jpn. 10 (1955) 794.

[7] Kazuo Suzuki, J. Phys. Soc. Jpn. 13 (1958) 179.

[8] A. Boatnera, E.P. Comera, G.W. Wrightc, J.O. Rameya, R.A. Riedeld, G.E. Jellison Jr., J.A. Kolopusa, Nuclear Instruments and Methods in Physics Research A 854 (2017) 82–88.